CHALMERS
UNIVERSITY OF TECHNOLOGY

Model Order Reduction Techniques for Physics-Based Lithium-ion Battery Management: A Survey

Downloaded from: https://research.chalmers.se, 2026-04-04 20:25 UTC

Citation for the original published paper (version of record):
Li, Y., Karunathilake, D., Vilathgamuwa, D. et al (2022). Model Order Reduction Techniques for Physics-Based Lithium-ion Battery Management: A Survey. IEEE Industrial Electronics Magazine, 16(3): 36-51. http://dx.doi.org/10.1109/MIE.2021.3100318

N.B. When citing this work, cite the original published paper.

© 2022 IEEE. Personal use of this material is permitted. Permission from IEEE must be obtained for all other uses, in any current or future media, including reprinting/republishing this material for advertising or promotional purposes, or reuse of any copyrighted component of this work in other works.

(article starts on next page)

Model Order Reduction Techniques for Physics-Based Lithium-Ion Battery Management: A Survey

Yang Li, Dulmini Karunathilake, D. Mahinda Vilathgamuwa, Yateendra Mishra, Troy W. Farrell, San Shing Choi, and Changfu Zou

To unlock the promise of electrified transportation and smart grid, emerging advanced battery management systems (BMSs) shall play an important role in health-aware monitoring, diagnosis, and control of widely used lithium-ion (Li-ion) batteries. Sophisticated physics-based battery models incorporated in the advanced BMS can offer valuable battery internal information to achieve improved operational safety, reliability and efficiency, and to extend the lifetime of the batteries. However, developed from the fundamental electro-chemical and thermodynamic principles, the rigorous physics-based models are saddled with exceedingly high cognitive and computational complexity for practical applications. This article reviews prevailing order reduction techniques of physics-based Li-ion battery models to facilitate the development of next-generation BMSs. We analyze and comparatively characterize these techniques, mainly from perspectives of model fidelity, computational efficiency, and the scope of applications. By representing many effective and flexible reduced-order models as equivalent circuits, designers and practitioners, who do not have electrochemical expertise but with knowledge of circuit theory, can readily gain insights into multi-physical dynamics as well as their coupling effects inside the batteries. In addition, recommendations are made on how to select appropriate physics-based models for various model-based applications in battery management. Finally, the prospect of physical model-enabled BMSs is discussed, including the potential challenges and future research directions.

I. Introduction to Li-ion Batteries and BMSs

A. Physics Behind Li-Ion Batteries

A typical Li-ion battery cell consists of many sandwich-like thin-layer structures. The structure is as depicted in Fig. 1: It comprises a porous positive electrode, a porous negative electrode, and a separator in between. The positive electrode contains various metal oxides or a mix of them, while the negative electrode is mostly graphite-based. In both electrodes, lithium ions are assumed to be stored in the lattice sites of the solid phase particles. The separator is an electronic insulator that allows the lithium ions to pass through. The electrodes and the separator are immersed in a concentrated solution of charged lithium ions named the electrolyte [1].

During the charging process, the lithium species in the solid phase of the positive electrode diffuse to the surface of the metal oxide particles, then react and transfer (de-intercalate) to the electrolyte as positively charged lithium ions. In the electrolyte, the charged lithium ions travel towards the negative electrode by means of diffusion and migration. On the surface of the negative electrode, the lithium ions react and

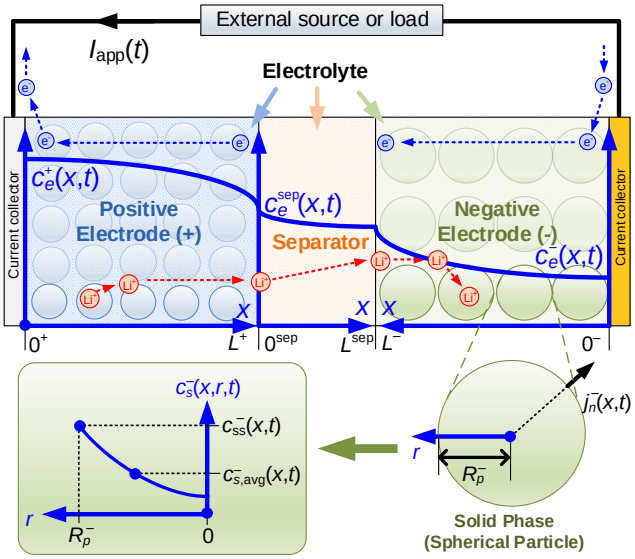

Fig. 1. Schematic of the sandwich-like structure of a typical Li-ion battery cell during the charging process.

intercalate into the graphite particles. At the same time, the insulated separator forces the electrons to flow in the opposite direction through the external electrical circuit connecting the current collector to a source. This de-intercalation/intercalation process is reversely applied when discharging to a load.

Apart from the intercalation/de-intercalation process, various side reactions occur in the cell and most of them are found to be detrimental to battery health. The major impact of the side reactions on battery performance is the loss of storage capacity and the increase of internal resistance, mainly caused by the growth of solid-electrolyte interphase (SEI) film and the deposition of metallic lithium, known colloquially as lithium plating. These side reactions occur most significantly at the separator/negative electrode interface [2], and they consume the active materials in the electrodes in an irreversible way, leading to reductions in cyclable lithium species and charge/discharge rate capability over time.

B. Vision of Advanced BMSs

It is essential for a BMS to accurately monitor the internal battery states so that judicious operational strategies and reliable fault diagnosis can be performed [3]. A well-managed Li-ion battery can slow down the aging of the battery cells, prevent cell failures, avoid catastrophic fire/explosions due to unintentional overcharging/over-discharging, over-temperature, external and internal short circuits of the cells, amongst other stressed operating states. Indicators such as the state-of-charge (SOC) and state-of-health (SOH) of battery are widely used in the existing BMS algorithms to signify the level of stored energy in the battery and the level of battery degradation [4]. These states can also be used to derive other information such as the remaining useful energy of the battery and power capability subject to operating limits placed on terminal voltage, maximum current rate, and allowable temperature range [5], [6]. In this way, the utilization of the battery capacity can be optimized to meet specific power control and energy management objectives [7], [8]. In addition, the BMS also tracks variations in battery parameters over time, detects degradation,

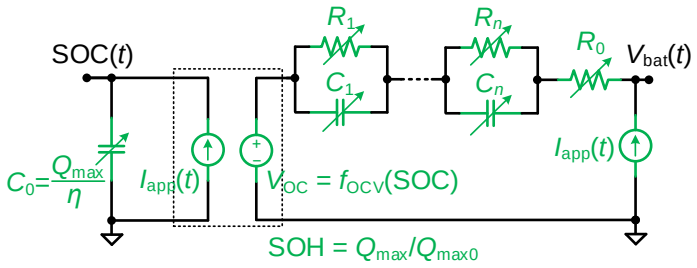

Fig. 2. A typical ECM of Li-ion batteries used in conventional BMSs. V_{bat}: Terminal voltage. I_{app}: Applied current. Q_{max}: Battery capacity. Q_{max0}: Battery capacity of a fresh cell. η: Coulombic efficiency. V_{OC}: Open-circuit voltage, expressed as a nonlinear function $f_{\text{OCV}}(\cdot)$ of the SOC.

maintains cell balancing, and takes countermeasures to restrain the development of faults and to prevent catastrophic failures so that the lifetime of the battery can be maximized [9].

However, none of the internal states and parameters can be directly measured: battery terminal voltage, current, and surface temperature are the only directly measurable quantities based on the prevailing sensor technologies. Therefore, a suitable mathematical battery cell model is often required in the design of model-based state/parameter estimators and control strategies [10], [11]. The battery model must be able to reproduce the cell dynamics with due considerations given to cell degradation, thermal effects, and parameter variations as the environmental and operating conditions change. Also, the battery model should be sufficiently accurate to reflect the nonlinearity and operating constraints, while computational efficiency and numerical stability of the model should be guaranteed for real-time implementation to achieve various control objectives [12].

C. Current Status and Challenges to Conventional BMSs

Nowadays, due to their mathematical simplicity, ease of implementation, and low-cost computation requirement, phenomenological equivalent circuit models (ECMs) have been the most commonly used tools in the development of the algorithms in the BMSs [11], [13]. In an ECM, battery electrochemical dynamic behaviors are emulated by an electrical circuit consisting of basic components such as capacitors, resistors, inductors, and controlled voltage/current sources. A widely adopted ECM with n parallel RC branches in the existing literature is illustrated in Fig. 2. Each of the circuit parameters, e.g., $R_0, C_0, R_1, C_1, \cdots, R_n$, and C_n, is expressed as a function of battery SOC and temperature, and identification of these functions requires a substantial number of offline tests and real-time tracking. Low-order empirically-based ECMs are affordable and well-suited to model batteries in existing applications that exhibit weak operating dynamics, e.g., supplying portable electronic devices, overnight charging of electric vehicles (EVs), and smoothing of renewable energy generation.

However, extrapolation beyond the observed data is problematic for the ECMs. The BMSs for emerging applications, such as extreme fast charging of electrified vehicles, need to be designed for higher current rates, increased dynamic load requirements, and harsher operating environments. Under these circumstances,

the model order, the complexity of the parameter functions, as well as the workload for experimental tests to identify the parameters, have to be increased drastically to achieve high model accuracy. [14]. Furthermore, as the circuit components do not bear direct relationships to the electrochemical processes occurring within the battery, the empirically-based ECMs tend to convey limited information on the physically meaningful time-varying parameters, degradation mechanisms, and internal safety constraints of the battery operation. The estimation of battery performance becomes erroneous if the evolving dynamic characteristics due to battery degradation are not properly taken into consideration. Furthermore, for full exploitation of the capability of the battery, ECMs are difficult to be adapted to control algorithms with a predictive model due to the lack of insight into how future behaviors are affected and aging and safety levels [15]. In view of these reasons, commercialized Li-ion battery systems are usually conservatively designed to allow for the high uncertainty in predicting the battery state and model parameters, rendering an increase in size, weight, and cost of the entire system.

II. First-Principle Model

To overcome the problems of the conventional ECMs and to fully exploit the potential of Li-ion batteries, it is beneficial for a sophisticated health- and safety-aware battery management strategy to adopt physics-based models derived from the fundamental electrochemical principles [14]. Based on the physical interpretation as presented in Section I-A, Doyle, Fuller, and Newman have introduced the basic multiscale modeling framework of the Li-ion batteries commonly referred to as the pseudo-two-dimensional (P2D) model or "DFN model" [16]–[18]. It consists of a set of partial differential algebraic equations (PDAEs) that describe the behaviors of several spatiotemporal variables including the Li-ion concentration c_s and potential Φ_s in the solid phase of the electrode, as well as the Li-ion concentration c_e and potential Φ_e in the electrolyte.

To uncover the common mathematical structure, the dynamic equations of the P2D model with 1D geometry can be generalized to the following partial differential equation (PDE) describing conservation laws:

$$M\frac{\partial u(z,t)}{\partial t} = \frac{1}{z^m}\frac{\partial}{\partial z}\left(z^m \delta \frac{\partial u(z,t)}{\partial z}\right) + \xi \tag{1}$$

subject to the boundary conditions at $z = z_1$ and $z = z_2$:

$$\alpha u(z_1,t) + (1-\alpha)\delta\frac{\partial u(z_1,t)}{\partial z} = \mathrm{BV}_1,$$
$$\alpha u(z_2,t) + (1-\alpha)\delta\frac{\partial u(z_2,t)}{\partial z} = \mathrm{BV}_2$$

and the initial condition at $t = 0$ if $M \neq 0$:

$$u(z,0) = u_0$$

where $u(z,t)$ represents a state variable of interest in the space $z \in [z_1, z_2]$ and at time $t \in [0,\infty)$; M is a coefficient that represents the capability to store a certain form of energy; δ is a coefficient signifying the rate of transport; ξ is the source term; u_0 is the initial value; BV_1 and BV_2 are two boundary values;

TABLE I

SUMMARY OF SYMBOLS IN THE P2D MODEL BASED ON THE GENERALIZED PDE (1)

Desciption	$u(z,t)$	z	m	M	δ	ξ	α	z_1	z_2	BV_1	BV_2	u_0	Eq.
Mass Transport (Solid Phase)	$c_s^+(x,r,t)$	r	2	1	$D_{s,\text{eff}}^+$	0	0	0	R_p^+	0	$-j_n^+$	c_{s0}^+	(2a)
	$c_s^-(x,r,t)$	r	2	1	$D_{s,\text{eff}}^-$	0	0	0	R_p^-	0	$-j_n^-$	c_{s0}^-	(2b)
Mass Transport (Electrolyte)	$c_e^+(x,t)$	x	0	ε_e^+	$D_{e,\text{eff}}^+$	$t_a^0 a_s^+ j_n^+$	0	0^+	L^+	0	$D_{e,\text{eff}}^{\text{sep}} \frac{\partial c_e^{\text{sep}}(0^{\text{sep}},t)}{\partial x}$	c_{e0}	(3a)
	$c_e^-(x,t)$	x	0	ε_e^-	$D_{e,\text{eff}}^-$	$t_a^0 a_s^- j_n^-$	0	0^-	L^-	0	$D_{e,\text{eff}}^{\text{sep}} \frac{\partial c_e^{\text{sep}}(L^{\text{sep}},t)}{\partial x}$	c_{e0}	(3b)
	$c_e^{\text{sep}}(x,t)$	x	0	$\varepsilon_e^{\text{sep}}$	$D_{e,\text{eff}}^{\text{sep}}$	0	1	0^{sep}	L^{sep}	$c_e^+(L^+,t)$	$c_e^-(L^-,t)$	c_{e0}	(3c)
Charge Transport (Solid Phase)	$\Phi_s^+(x,t)$	x	0	0	σ_{eff}^+	$Fa_s^+ j_n^+$	0	0^+	L^+	$-I_{\text{app}}/A$	0	–	(4a)
	$\Phi_s^-(x,t)$	x	0	0	σ_{eff}^-	$Fa_s^- j_n^-$	0	0^-	L^-	I_{app}/A	0	–	(4b)
Charge Transport (Electrolyte)	$\Phi_e'^+(x,t)$	x	0	0	κ_{eff}^+	$-Fa_s^+ j_n^+$	0	0^+	L^+	0	$-I_{\text{app}}/A$	–	(5a)
	$\Phi_e'^-(x,t)$	x	0	0	κ_{eff}^-	$-Fa_s^- j_n^-$	0	0^-	L^-	0	I_{app}/A	–	(5b)
	$\Phi_e'^{\text{sep}}(x,t)$	x	0	0	$\kappa_{\text{eff}}^{\text{sep}}$	0	0	0^{sep}	L^{sep}	$-I_{\text{app}}/A$	$-I_{\text{app}}/A$	–	(5c)

$\alpha \in \{0,1\}$ is a coefficient to determine the type of the boundary conditions; and m indicates the type of coordinates associated with the PDE. As shown in Fig. 1, when $m = 0$, (1) describes the transport and conduction phenomena along the horizontal direction of the cell on the macroscale ($z = x$), while the dynamics along the remaining two dimensions perpendicular to x are ignored. For $m = 2$, (1) describes the transport of the lithium species along the pseudo spherical dimension ($z = r$) on the microscale. Note that the case of $m = 1$ describes the dynamics in a cylindrical coordinate whereas it is not used in the original P2D model.

Table I summarizes the symbols defined for different governing equations in the P2D model, where the superscripts "+", "−", and "sep" represent the positive electrode, negative electrode, and separator domains, respectively. For ease of notation, we use $\pm \in \{+,-\}$ and $j \in \{+,-,\text{sep}\}$ to indicate the quantities in different domains. Specifically, $j_n^\pm$ is the pore-wall molar flux between the solid phase and the electrolyte; L^j is the width of a domain; ε_e^j is the volume fraction of the electrolyte; t_a^0 is the transference number; F is the Faraday constant; A is the cross-sectional area of the electrode; and $c_{s0}^\pm$ and c_{e0} are the initial concentrations of the solid phase and the electrolyte, respectively. Parameters such as the solid-phase and electrolyte diffusivities ($D_{s,\text{eff}}^\pm$ and $D_{e,\text{eff}}^j$) as well as the solid-phase and electrolyte conductivities ($\sigma_{\text{eff}}^\pm$ and κ_{eff}^j) are usually concentration- and/or temperature-dependent. In addition, as indicated in Fig. 1, $R_p^\pm$ represents the radius of the assumed spherical particle in the solid phase, and $a_s^\pm = 3\varepsilon_s^\pm / R_p^\pm$ represents the specific electrode area, where $\varepsilon_s^\pm$ is the volume fraction of the solid phase. In (5), instead of using electrolyte potential Φ_e^j to describe the charge transport as in the original P2D model, a new potential term

$\Phi_e'^j$ is defined based on (6), so that the corresponding PDE can be written in the generalized form (1) [19].

$$\Phi_e'^j(x,t) := \Phi_e^j(x,t) - \overbrace{\left(\frac{2R_gTt_a^0}{F}\right)\ln\left(\frac{c_e^j(x,t)}{c_{e0}}\right)}^{U_e^j(x,t)} \tag{6}$$

where R_g and T are the universal gas constant and the cell temperature, respectively. The term U_e^j is an overpotential due to the deviation of electrolyte concentration from its initial value c_{e0}, and we denote this nonlinear relationship as $U_e^j = f_E(c_e^j)$.

Next, the Butler-Volmer equation is used to describe the intercalation reaction kinetics during charging and discharging. It establishes a nonlinear coupling relationship between the ionic molar flux $j_n^\pm$ and the charge-transfer overpotential $\eta_{\text{ct}}^\pm$ in the corresponding electrode

$$j_n^\pm(x,t) = i_0^\pm(x,t)\left[\frac{2}{F}\sinh\left(\frac{F\eta_{\text{ct}}^\pm(x,t)}{2R_gT}\right)\right] \tag{7}$$

$$\eta_{\text{ct}}^\pm(x,t) = \Phi_s^\pm(x,t) - \Phi_e^\pm(x,t) - U_{\text{ss}}^\pm(x,t) - Fr_f^\pm(x,t)j_n^\pm(x,t) \tag{8}$$

where the reaction current density $i_0^\pm$ is expressed as a nonlinear function of $c_{\text{ss}}^\pm$ and $c_e^\pm$, $r_f^\pm$ represents the area-specific film resistance of the SEI layer, and $U_{\text{ss}}^\pm$ is the open-circuit potential (OCP) of the electrode. Denoting the Li-ion concentration at the surface of the solid particle as $c_{\text{ss}}^\pm(x,t) := c_s^\pm(x, r = R_p^\pm, t)$, $U_{\text{ss}}^\pm$ can be expressed as a nonlinear function of $c_{\text{ss}}^\pm$, i.e., $U_{\text{ss}}^\pm = f_{\text{OCP}}^\pm(c_{\text{ss}}^\pm)$. This function is determined by the thermodynamic characteristics of the active materials used in the electrode.

Finally, the terminal voltage and SOC of the battery are obtained by

$$V_{\text{bat}}(t) = \Phi_s^+(0^+,t) - \Phi_s^-(0^-,t) + R_{\text{col}}I_{\text{app}}(t) \tag{9}$$

$$\text{SOC}(t) = \frac{1}{L^-}\int_{0^-}^{L^-}\left[\frac{3}{\left(R_p^-\right)^3}\int_0^{R_p^-} r^2\frac{c_s^-(x,r,t)}{c_{s,\max}^-}dr\right]dx \tag{10}$$

where R_{col} is the lumped resistance of the current collectors and $c_{s,\max}^-$ is the theoretic maximum concentration in the negative electrode. Readers are referred to [14], [19], [20] for more detailed descriptions of the P2D model.

The P2D model described by (1)–(10) is very general and modifications can be made to accommodate Li-ion batteries of different types of chemistry, such as lithium cobalt oxide (LCO) [21], lithium iron phosphate (LFP) [22], lithium manganese oxide (LMO) [17], lithium nickel cobalt aluminum oxide (NCA) [23], and lithium nickel manganese cobalt oxide (NMC) [2], [24].

Besides the intercalation/de-intercalation process described in (1)–(10), different side-reaction models can be incorporated into the P2D framework to predict aging phenomena such as the increase of the resistance due to SEI film growth and strain-induced cracking of the solid particles, the decrease in the electrolyte volume fraction, as well as the capacity fade due to the SEI film growth and lithium plating, and relevant parameters can be used to define the SOH of the cell [25]. For example, the driving force of lithium plating, called the side reaction potential, can be modeled by an equation similar to (8) [2], whereas it is inherently difficult for conventional ECMs to distinguish and capture these localized aging characteristics. Therefore,

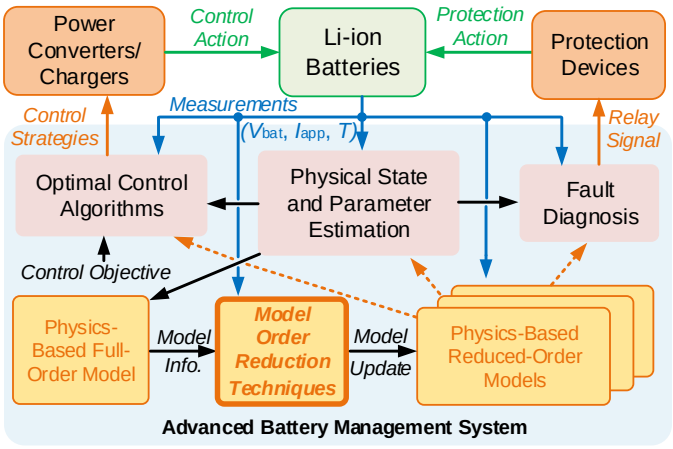

Fig. 3. Structure of an advanced BMS. Physics-based reduced-order models are used for basic BMS functions including state/parameter estimation, fault diagnosis, and determination of the optimal control algorithms. The state/parameter estimation guarantees that the physics-based model is sufficiently accurate over its entire operational lifetime. The optimal control algorithm block uses the model information and the control objective to calculate the optimal current profile for the battery. The fault diagnosis algorithm utilizes the estimated faulty state/parameters information to direct the protection system.

the P2D model and its extension to corporate aging dynamics are favorable to the development of advanced BMSs, potentially leading to extended battery life.

III. Model Order Reduction Techniques

Model order reduction (MOR) techniques can be adopted to obtain simplified first-principle Li-ion battery models. The rapid pace of advancement in microprocessor technology has enabled the implementation of high-fidelity reduced-order models (ROMs) of the Li-ion battery with over 100th system order [24], which has the potential to be incorporated in real-time embedded systems as a "digital twin" of the battery [26]. However, model orders not much higher than that of the prevailing ECMs with 2 to 5 states [27] are most desirable in the design of many BMS functionalities, such as online state estimation [28], available power prediction [29], parameter estimation [30], cell balancing [31], and fault diagnosis [32]. The development of optimal battery control, such as the fast charging for EVs, energy management for HEVs, and power flow control for grid-connected battery energy storage systems, also requires a low-order system to balance the trilemma of high charging/discharging rates, long battery life, and ensured safety, since the complexity of most of those algorithms increases dramatically as the order of the model increases [33]. A schematic diagram of an advanced BMS with physics-based ROMs is shown in Fig. 3.

Extensive efforts have been made in developing MOR techniques in applied mathematics. However, for control-oriented MOR of Li-ion batteries, intuition-based techniques reported in the existing literature are also very effective since they avoid complex numerical re-calculation of ROM parameters, necessitated by battery degradation and nonlinearity. These ROMs can be implementable in real-time control algorithms [10]. The main control-oriented MOR techniques applied to the P2D model will be discussed in four categories next. A large proportion of the methods can be visualized and explained by reformulating the

ROMs into physically meaningful equivalent circuits [19], [34], [35], so that better understanding and more insights can be gained for the readers with a background in electrical and electronic engineering.

A. Spatial Discretization

The most straightforward and mathematically mature direction to simplify a PDAE system is to first employ discretization in the spatial coordinate ($z = x$ or r) to obtain a continuous-time differential-algebraic equation (DAE) system. The DAEs are next discretized in the time domain for online implementation. This strategy is usually referred to as the *method of lines*. The finite difference methods (FDM) [36] and the finite volume methods (FVM) [37] are the most direct methods in this category to simplify the equations (3)–(5) that govern the macroscale variables. For the solid-phase diffusion equation (2) established in the pseudo spherical coordinate, the method of lines can also be used via FDM [38], FVM [39], or the control volume method [40], etc. In FVM and the control volume method, the law of mass conservation has been specifically guaranteed so that no drift effect occurs during long-running operations.

By applying spatial discretization to (1), a general coupled circuit network that exhibits the distributed-parameter nature of the P2D model can be obtained using electrical analogy as shown in Fig. 4, where a subscript i is attached to indicate the variable at the ith mesh node or control volume while the superscript to indicate the domain is dropped. This transmission-line-like general circuit representation consists of a subcircuit for the charge transport process as shown in Fig. 4(a), a subcircuit for the mass transport process in the electrolyte as shown in Fig. 4(b), and a set of subcircuits for the mass transport in the solid phase of the electrodes as shown Fig. 4(c). These subcircuits interact with each other by the coupling components depicted in Fig. 4(d). Note that the battery degradation is closely related to the voltage $\Phi_{s,i} - \Phi_{e,i}$ and the resistance $R_{\Sigma,i}$ on the vertical branches in Fig. 4(a). Here, $R_{\Sigma,i}$ consists of the local SEI resistance $R_{\text{SEI},i}$ (which is proportional to r_f in (8)) and the intercalation-related charge-transfer resistance defined as $R_{\text{ct},i} := \eta_{\text{ct},i}/I_{n,i}$, where $I_{n,i} = Fa_{s,i}j_{n,i}\Delta x_i$ is the branch current and Δx_i represents the discrete space interval in the x-direction. During battery operation, various side reactions occur which causes battery performance to deteriorate due to the increase of the resistance $R_{\text{SEI},i}$ and loss of cyclable lithium. The rates of side reactions are mainly affected by the magnitude of the value of $\Phi_{s,i} - \Phi_{e,i}$. Therefore, accurate modeling of the degradation behaviors such as those associated with $R_{\text{SEI},i}$ and $\Phi_{s,i} - \Phi_{e,i}$ is beneficial for battery health monitoring, diagnosis, and optimal control.

The spatial discretization methods can preserve most model properties within a wide range of operating conditions and model extension can be readily achieved to consider the nonuniformity of the double-layer capacitance [34], mechanical stress [41], heat accumulation and transfer [21], aging behaviors [2], [34], etc., on different time scales. The capability to retain the slow dynamics during the relaxation process is another distinguishing feature for these approaches, i.e., after the current I_{app} is removed, the capacitor voltages in Figs. 4(b) and (c) shall be gradually equilibrated through a chain of interactions between subcircuits. Clearly, the complexity and the accuracy of these ROMs are determined by the number and the positions

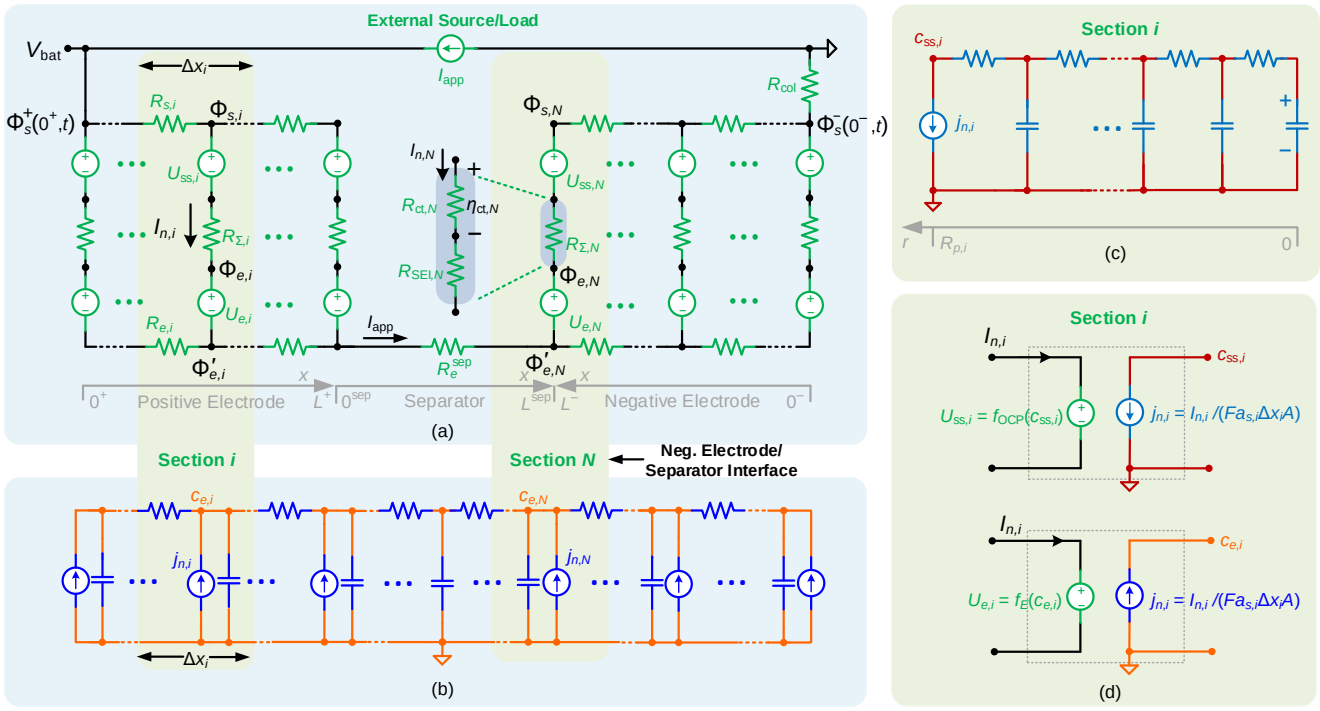

Fig. 4. General distributed-parameter equivalent circuit for the pseudo-two-dimensional (P2D) model obtained by spatial discretization: (a) Subcircuit for charge transport and intercalation/de-intercalation reaction kinetics. (b) Subcircuit for mass transport in the electrolyte. (c) The subcircuit in the ith section (node) in the macroscale for mass transport in the solid phase of the electrode. (d) Coupling between the charge and mass transport subcircuits on the ith section (node) on the macroscale.

of the mesh points/control volumes of interest. Uneven nodes can be used to increase the model fidelity [40]. Using FVM, the simulation results in Fig. 5(a) show that only a small number of discretized points are required under the operating condition with low current rates. However, as the current increases, from Fig. 5(b), it can be seen that more nodes are needed to reproduce the inflated (or compounded) distributed effects and characteristics due to saturation of concentrations. This would be difficult both for model-based control system design and online implementation. MORs for large-scale interconnected circuit networks have the potential to further reduce the order of the discretized battery model [42].

B. Function Approximation

The second category of methods approximates the spatiotemporal variables by a finite weighted sum of assumed functions in the form of

$$u(z,t) \approx \sum_{k=0}^{N} \alpha_k(t) f_k(z) \tag{11}$$

The objective of such methods is to find the time-varying coefficients $\alpha_k(t)$ for the selected *trial functions* (or *basis functions*) $f_k(z)$, so that the residual $\mathcal{R}(z,t) = u(z,t) - \sum_{k=0}^{N} \alpha_k(t) f_k(z)$ has certain properties which allow one to minimize the errors in the approximation. The trial functions are usually selected as constant, power, sinusoidal, logarithm, polynomial, or a combination of them, and usually to ensure the boundary conditions are automatically satisfied. They are sometimes referred to as the projection-based

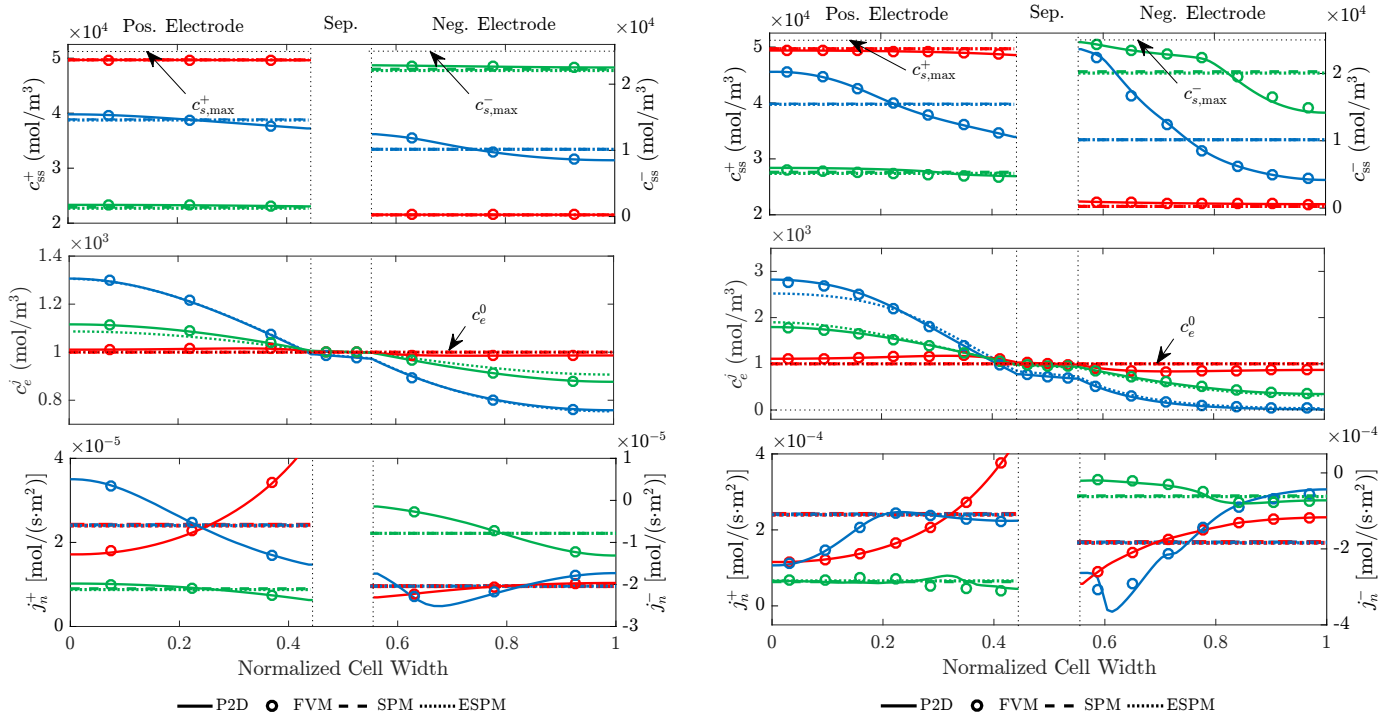

(a) (b)

Fig. 5. Comparison of the spatial distributions of solid-phase surface concentration ($c_{ss}^{\pm}$), electrolyte concentration (c_e^j), and pore-wall molar flux ($j_n^{\pm}$) simulated using different models during a constant-current constant-voltage (CC-CV) charging process. The CC stage is with (a) a low current rate and (b) a high current rate. Red: Early CC stage. Blue: Late CC stage. Green: CV stage. Solid line: P2D model. Circle: Discretized model using FVM. Dashed line: SPM. Dotted line: ESPM.

methods, where the trial functions and weights can be obtained via optimization, e.g., by minimizing the Euclidean norm error in the frequency domain [43], or via applying eigenfunction/singular value decomposition to a data ensemble obtained from the full-order model [39].

A broad category of these methods is known as *spectral methods*, where the integral of the weighted residual over the domain $[z_1, z_2]$ of z should vanish, i.e.,

$$\int_{z_1}^{z_2} w_k(z)\mathcal{R}(z,t)dz = 0 \quad k \in \{0, 1, \cdots, N\} \tag{12}$$

where the weights $w_k(z)$ are called *test functions*. In the Galerkin methods [44], the test functions equal the trial functions $f_k(z)$. Cosine functions [44], Chebyshev polynomials [45], and Legendre polynomials [46], [47] are usually chosen as the trial or test functions in the spectral methods due to their good characteristics for non-periodic signal reconstruction. In the orthogonal collocation methods or pseudospectral methods [45], [48], [49], the test functions are the Dirac delta functions defined at specific locations (namely, the collocation points). The accuracy of the spectral methods can be improved with increased approximation order N, but at the expense of drastically increased complexity in deriving the ROM analytically.

With the consideration of constraints such as the boundary conditions, conservation of mass, and geometrical properties of the solution, heuristic methods can also be used to select the trial functions to simplify the determination of the coefficients. Only a small set of trial functions need to be used so that the

resulting model can be explicitly expressed as functions of battery parameters. For example, in approximating the solid-phase concentration PDE (2), the solid-phase concentration $c_s^{\pm}$ can be assumed as a polynomial function of the radial position r with only even-degree terms. The coefficients $\alpha_k(t)$ in (11) are obtained as functions of several physically meaningful quantities, such as the volume-averaged concentration $c_{s,\text{avg}}^{\pm}$ and the volume-averaged concentration flux, as well as the surface concentration $c_{\text{ss}}^{\pm}$. This leads to a two- or three-parameter polynomial profile approximation [50], which can be illustrated using the equivalent circuit shown in Figs. 6(a) and (b), respectively. This method is valid when the effective diffusion coefficient $D_{s,\text{eff}}^{\pm}$ of the solid phase is either a constant or a function of the solid-phase concentration [51], and they perform well under constant, long-time, low-to-medium current-rate applications. However, there can be significant approximation errors under high current-rate and/or high-frequency applications such as fast charging for EVs [52], pulse operations of hybrid electric vehicles (HEVs) [53], and the provision of fast frequency response for grid systems [54]. Higher-order approximations are needed so as to more accurately describe the increased spatial nonuniformity in the solid particles. The polynomial profile concept has also been applied to the approximation on the macroscale for the electrolyte concentration and potential [55], molar flux, solid-phase concentration, and conductivity of electrolyte [21]. However, on this macroscale, the polynomial profile assumption can fail during dynamic operation at high rates or at the end of the charge/discharge process. For example, in the application of fast charging, the local solid-phase concentration near the separator and the local electrolyte concentration tend to saturate or close to their physical or safety limits, and the low-order approximation is unlikely to be precise to approximate the situation. A high-order approximation is needed for such conditions, while the derivation of the coefficients can be much more complicated.

C. Frequency-Domain Approximation

Transfer functions are essentially control-oriented and can be readily realized in state-space forms for linear control system design. For the MORs techniques under this category, the main objective is to find a rational transfer function between the input current I_{app} and the local variable of interest, such as the local concentrations or overpotentials. As (1) represents an infinite-order system, the transfer function between any state u and the input (the source ξ or a boundary value, see Table I) is transcendental. For example, the analytical result for the solid-phase diffusion equation (2) can be obtained by using Laplace transform to (1) with the consideration of its boundary conditions, i.e. [27],

$$\frac{c_{\text{ss}}^{\pm}(x,s)}{j_n^{\pm}(x,s)} = \frac{R_p^{\pm}}{D_{s,\text{eff}}^{\pm}} \frac{\tanh\left(R_p^{\pm}\sqrt{s/D_{s,\text{eff}}^{\pm}}\right)}{\tanh\left(R_p^{\pm}\sqrt{s/D_{s,\text{eff}}^{\pm}}\right) - R_p^{\pm}\sqrt{s/D_{s,\text{eff}}^{\pm}}} \tag{13}$$

However, as the equations in the P2D model are highly nonlinear and tightly coupled, additional steps are needed to identify the relationship between the current I_{app} and the local molar flux j_n (which is proportional to the branch current $I_{n,i}$ shown in Fig. 4(a)). Assumptions are usually made to decouple the submodels, e.g., by assuming a spatially uniform molar flux distribution $(j_n^{\pm}(x,t) = \pm I_{\text{app}}(t)/(Fa_s^{\pm}L^{\pm}A))$ in the electrode, and/or considering constant electrolyte concentrations $(c_e^j(x,t) = c_{e0})$ [27].

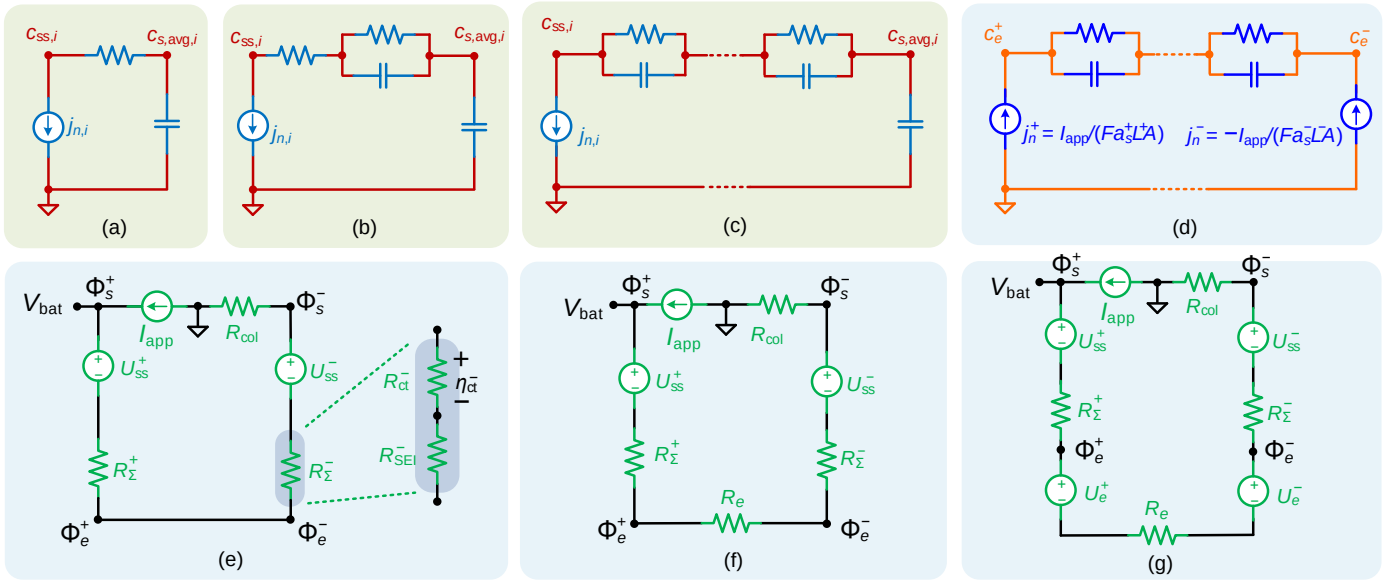

Fig. 6. Equivalent circuits to (a) two-parameter polynomial approximation, (b) three-parameter approximation, (c) diagonal canonical form realization of Padé approximation, residue grouping, etc., obtained using the diagonal canonical realization. (d) electrolyte concentration dynamics based on Padé approximation and uniform molar flux, (e) single particle model, (f) electrode averaged model, and (g) single particle model with electrolyte.

Next, MOR methods are applied to the transcendental transfer functions to find the rational transfer functions as required. Among various MOR methods, the eigenfunction method calculates all the periodic roots of the transcendental transfer function analytically, and the resulting infinite series will be truncated to obtain a ROM [56]. Similarly, in the residue grouping method, all periodic poles and zeros will be calculated and truncated, while these poles will be first grouped and approximated with new ones by minimizing a frequency response cost function using nonlinear optimization techniques [27]. Compared to the eigenfunction method, the residue grouping method can offer improved accuracy of frequency response in a wide range. However, the residue grouping method is less implementability for real-time systems as it is computationally inefficient, sensitive to initial guess, and there is no guaranteed convergence and global optimality. In contrast, in the Padé approximation, the transcendental transfer functions are linearized into rational ones in the s-domain, so that the system order can be directly reduced by moment-matching [57]. The coefficients of these rational polynomials consist of physical parameters of the cell and can be updated readily according to any change in the operational condition. Accuracy is further improved by increasing the order of the rational transfer functions used in the approximation. There is a trade-off between the required level of accuracy and the computational overhead, as the increase in model order eventually imposes additional computational requirements. Low-order Padé approximations provide sufficiently accurate results for stationary battery applications, and higher-order ones can be used for EV applications [58].

A transfer function can be expressed in different impedance forms, depending on the realization strategies to obtain a state-space model. For the solid-phase diffusion equation (2), a general equivalent circuit based on diagonal canonical realization is presented in Fig. 6(c), where the surface concentration $c_{\mathrm{ss},i}$ is expressed

as the sum of the volume-averaged concentration $c_{s,\text{avg},i}$ and a series of concentration deviation terms. With the uniform molar flux assumption, a circuit for the electrolyte diffusion equation (3) can be derived and is shown in Fig. 6(d). Similar to the method of lines presented in Section III-A, the continuous-time ROMs obtained from the residue grouping and the Padé approximation need to be discretized in the time domain for control system implementation. In contrast, the dynamic realization algorithm generates an optimal reduced-order discrete-time state-space realization from the original PDE directly, by first finding the discrete-time pulse response, and then using the Ho-Kalman algorithm to compute the state-space realization [59]. Several improved linear discrete-time models based on such a realization process are investigated and compared in [60], where it concludes all of them are more computationally efficient than the dynamic realization algorithm with less memory requirement, although it is difficult to relate the model parameters directly to any physical meanings [45].

The derivation of the ROMs from the frequency domain analysis is usually labor-intensive, although the resulting models are easy to implement once obtained. Since it is only necessary to evaluate the variables at specific locations of interest within the battery, the computational burden can be lower than the spatial discretization methods where all locations need to be considered at the same time. However, as there is no guarantee that the transfer functions for different variables share the same poles, the order of the ROMs can be high to achieve high model precision if a large number of internal variables need to be investigated simultaneously. Furthermore, as some assumptions and linearization steps are taken in such small-signal methods, the fidelity of the ROMs can be low in extreme operating conditions with persistent current rates applied, such as during fast charging. Relaxing the assumptions of small perturbation can lead to much more complex modeling processes [61].

D. Simplified Physics/Spatial Lumping

In many physics-based Li-ion battery ROMs, assumptions are made by fully or partially ignoring the macroscale dynamics effects under specific operating conditions. In the electrode, it leads to a uniform molar flux and such an assumption has been extensively adopted in combination with the techniques in the previous categories, e.g., those described in Sections III-B and III-C. By this means, the complex physical dynamics and strong coupling relationships between different submodels can be significantly simplified.

The single particle model (SPM) assumes uniformity for all local variables in each electrode, and the negligible impact of the variation of electrolyte concentration and potential on terminal voltage [51]. This assumption tends to be valid under relatively low current rates and/or for cells with thin electrodes. To illustrate, one can consider that in Fig. 4(a), when the electrode is very thin, or if the injected current rate and thus the branch currents flowing through the solid-phase resistance $R_{s,i}$ and electrolyte resistance $R_{e,i}$ are low. This results in negligible differences in the local potentials and currents. In addition, under the assumption $c_{e,i} = c_{e0}$, the voltage sources $U_{e,i}$ can be deleted from the circuit since according to (6), $U_{e,i}$ is proportional to $\ln(c_{e,i}/c_{e0})$. This renders a simplified lumped-parameter ECM for the SPM, as shown in

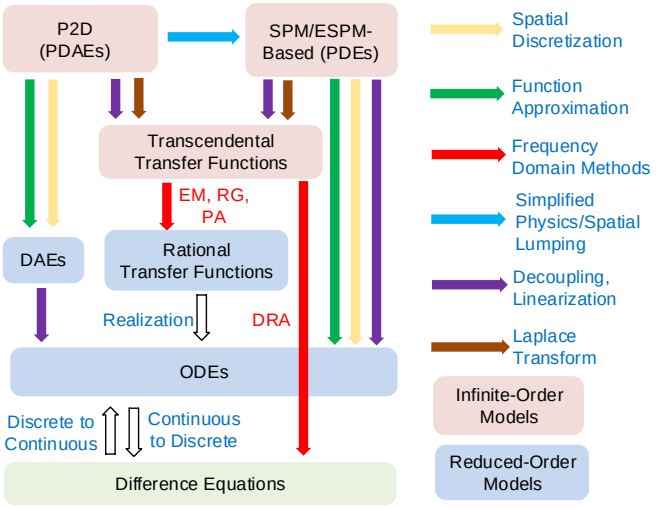

Fig. 7. Relationships between major MOR techniques for the P2D model. EM: eigenfunction methods. RG: residue grouping. PA: Padé approximation. DRA: dynamic realization algorithm.

Fig. 6(e). In the literature, it shows that the maximum applicable current rate is usually 1C[1] for a high-power type battery with thin electrodes, and 0.5C for a typical high-energy battery that has a wider electrode [14]. Hence, the SPM is generally not recommended for high-power applications, such as fast charging for EVs and HEV operation with high power pulses involved [14], but it is well-suited for many grid applications [62], [63] and daily driving activities of EVs, where the required operating ranges are much narrower.

Similar to the SPM, an electrode averaged model was developed in [38] by averaging the distributed variables in the electrodes. It couples the average solid material concentration with the average values of the chemical potentials, the electrolyte concentration, and the current density, as shown in Fig. 6(f). The electrolyte dynamics are considered to be sufficiently fast compared to the diffusion process in the electrodes and therefore, they can be modeled as purely resistive in nature as shown in Fig. 6(f). The electrolyte concentration is considered to be constant for electrochemical state observer design [64]. Further improvement of the SPM or the electrode averaged model was made by adding the effect of the distributed electrolyte concentration and potential variations. For example, the enhanced or extended SPM [55], [65] and the SPM with electrolyte [66], denoted by ESPMs in general in this work, are all developed based on the concepts of spatially lumping certain quantities. They can be illustrated using the ECM shown in Fig. 6(g), where the impact of the electrolyte concentration variation and electrolyte potential is embodied by lumped voltage source $U_e^{\pm}$ and electrolyte resistance R_e.

IV. Comparison of MOR Techniques

In the literature, the four categories of MOR methods presented in the previous section have all been applied to achieve various BMS functionalities including state/parameter estimation, fault diagnosis, and

[1]1C current rate is defined as the current through the battery divided by the theoretical current draw under which the battery would deliver its nominal rated capacity in one hour. It has the units of h^{-1}.

optimal control. The relationships between these different MOR methods are shown in Fig. 7, and the typical methods, strengths and weaknesses, as well as their possible applications are summarized in Table II. From this table, it is observed that the spatial discretization methods are the most direct and widely applicable techniques to obtain accurate results, and the model accuracy can be improved by increasing the number of discretization nodes or control volumes. For some of the function approximations, it is possible to increase the fidelity of the ROM by assuming a more complex basis function with higher order. A spectral method can achieve the same accuracy as a discretization method with much fewer discretization nodes, typically with a reduction factor of 10 to 100, provided the solution is sufficiently smooth in the space domain [45]. As for the frequency-domain techniques, the derivation procedures are considerably more complex, especially for obtaining the transcendental transfer functions. Matching a wide frequency range also requires high-order approximations. Since the frequency-domain methods rely heavily on the assumption that the system is linear, the accuracy cannot be enhanced much in situations when large signals are involved. However, the methods can be very suitable for applications in which the battery is cycling about a specific level in the mid-SOC region, such as HEV and grid frequency control. Regarding the uniform assumption on spatially distributed variables, should this assumption prove to be invalid, it is impossible to increase the accuracy of the ROMs by increasing the model orders. The SPM is one of the most simplified frameworks of the electrochemical model, requiring very low computation but providing sufficient model accuracy for applications limited to low or medium current rates. It can be considered as a special case of the spatial discretization models with only one control volume or node for each electrode. The ESPMs are introduced to enhance the SPM by incorporating concentration and potential variations inside the cell. As a result, the span of applicability of the ESPMs is increased by providing sufficiently accurate results under high current rates and with a substantially less computational burden compared to the P2D model. In a practical ROM, the above four categories of MOR techniques are usually blended. This is because a combination of them can potentially offer an improved balance between model accuracy and computational complexity. In addition, prior knowledge on physical constraints and assumptions, such as the shape of the solution, the conservation of mass and charge, the satisfaction of the boundary conditions, volume-average values, and continuity, etc., are all useful for developing a proper ROM for a specific application.

Special consideration for the ROMs of the P2D model should be paid to the Butler-Volmer equation (7) as it imposes an algebraic constraint in the P2D model. This adds to computation difficulty in solving the model if the ROMs are DAEs, since in each time step, an iterative method has to be used to obtain a reasonably accurate solution. Linearization is often used to remove such an algebraic constraint with an approximated charge-transfer resistance R_{ct}, and this is essentially carried out in the frequency-domain methods.

As an example, Fig. 8 compares the frequency response and time-domain pulse current response for the solid-phase diffusion equation (2b) using several typical MOR techniques, and in the legend, the number in the parentheses indicates the model order. In Fig. 8(a), the ideal frequency response is calculated using the

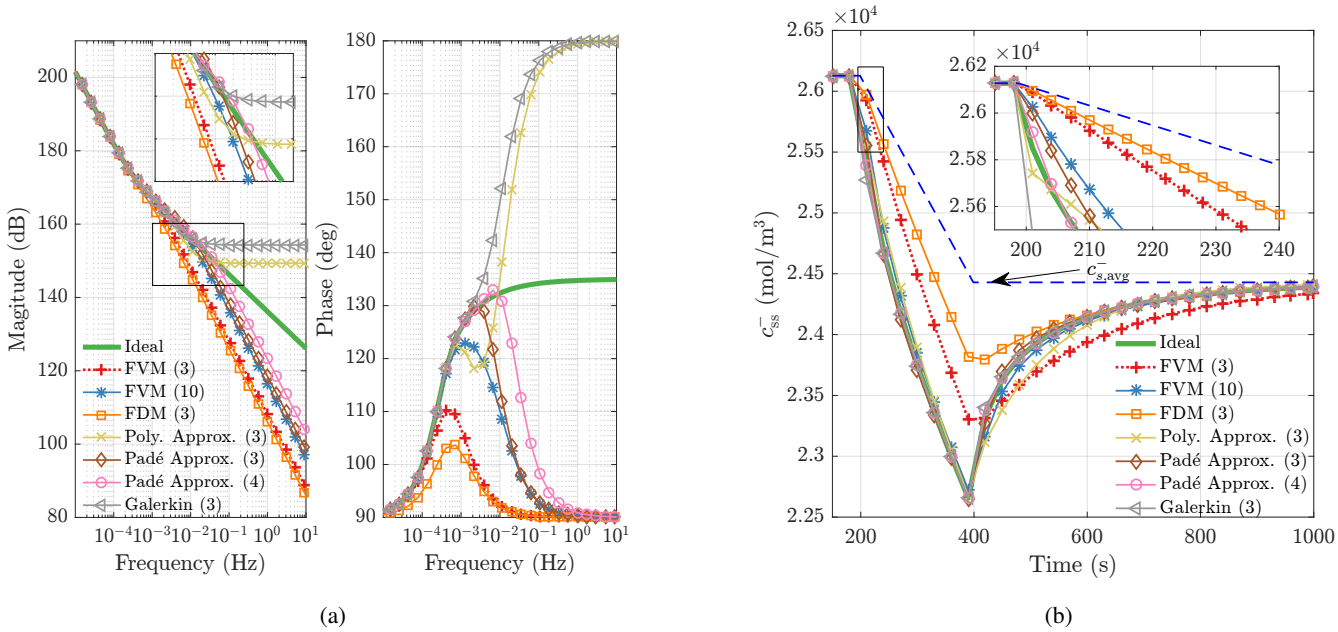

Fig. 8. Comparison of different MORs applied to the solid-phase diffusion equation (2b) of the negative electrode: (a) Frequency response. (b) Transient of the surface concentration under 1C pulse discharging current. In the legend, the number in the parentheses indicates the model order. Parameters used for the simulation: $R_p^- = 4 \times 10^{-6}$ m, $D_{s,\text{eff}}^- = 3.9 \times 10^{-15}$ m^2/s, $c_{s,\text{max}}^- = 30,555$ mol/m^3. The magnitude of the molar flux pulse between 200 s and 400 s is $j_n^- = -1.13 \times 10^{-5}$ mol/(m$^2 \cdot$ s).

transcendental transfer function (13), and it shows that most ROMs can capture the characteristics in the low-frequency region with very low-order approximation, while the system order has to be increased for a wider range of frequency response. In this example, the Padé approximation has shown superior effectiveness compared to the spatial discretization methods and the function approximation methods: the 3rd-order Padé approximation outperforms all other tested ROMs of the same model order and it is even more accurate than 10th-order FVM. However, the results cannot be simply extrapolated to the full P2D model, since the fidelity of the MORs can be significantly affected by other governing equations and parameters.

In the literature, the feasible operating range of a ROM is usually indicated by the maximum applicable current rate, provided certain requirement on model accuracy (e.g., voltage errors) is met. However, since the efficacy of an MOR technique heavily depends on the underlying assumptions imposed on the battery parametric values under specific operating conditions, when developing a ROM for BMS functions, it is less rigorous to select the MOR techniques simply based on the conclusions drawn from such a comparison of current rates. Instead, a general procedure to select suitable MOR techniques for deriving a ROM in BMS applications is suggested as follows.

1) Obtain prior knowledge of the battery's characteristics. The information includes the type of cell chemistry, the rate capability, and the parameter set of the physics-based model.

2) Identify the operating conditions and the characteristics of the current or power profiles, e.g., the maximum magnitude and the bandwidth (frequency range) of the current. For the applications where the Li-ion battery is likely to work closer to its endurance limits, the nonuniform behaviors in the electrode

become more significant, and thus a higher-dimensional ROM might be needed.

3) Select an infinite-order model as the benchmark, which can be a PDE- or a PDAE-based model, such as the P2D model, SPM, and ESPMs as indicated in Fig. 7. Simulate the benchmark model based on the selected input current profiles for specific applications. Obtain the computed results of the battery variables of interest (time series or spatial profile) which are to be used to validate the accuracy of the ROM. Make assumptions based on the simulation results.

4) Select MOR methods and apply the algorithms to a submodel of the P2D model. Perform the simulation using the reduced-order submodels and then compare the simulation results with that obtained using the benchmark model.

5) Evaluate the performance of the whole ROM by comparing it with the full-order model.

The readers are referred to existing simulation tools for algorithm development and performance evaluation of the ROMs with the P2D model being the benchmark, including commercial software MATLAB/Simulink, COMSOL Multiphysics, GT-AutoLion, as well as open-source packages such as DUALFOIL (Fortran) [67], fastDFN (MATLAB) [68], LIONSIMBA (MATLAB) [20], and PyBaMM (Python) [69].

V. Challenges and Outlook

A. Pack-Level Physics-Based Models

Owing to the power and capacity limits of individual cells, a large number of them have to be connected in series and in parallel to meet high-power and high-energy requirements in many practical applications. However, even new battery cells of the same type have inevitable variations in terms of capacity, internal resistances, or SOC among other parameters due to imperfections in the manufacturing process. Such cell inconsistencies may be amplified and propagated during the subsequent battery operations. The performance of the battery pack is therefore different from simply adding up each in-pack cell's performance. In fact, the pack performance is usually limited by the weakest cell. When implementing particular battery models in the BMS, appropriate parametric values of the physics-based model need to be selected consistent with the different types of battery chemistry. The sophisticated physics-based pack-level battery models will require high computational power and large memory capacities to store the processed data. Moreover, in practice, the inconsistencies amongst cells may create electrical imbalances [106], and as such, additional circuitry [107] or controlling mechanisms [31], [78] are required to overcome the problem. Therefore, there is a strong need to develop efficient physics-based pack-level battery models to deal with cell inconsistency. Furthermore, the obtained models must be computationally efficient in order to cater to online applications. The pack-level physics-based modeling poses a technical challenge in front of advanced BMSs. On the other hand, addressing the problem means all the benefits of physics-based models can be scaled up to fundamentally improve the battery performance. This is considered to be one of the future research topics and solicits expertise in electrochemistry, mathematical modeling, and computational science.

TABLE II

STRENGTHS, WEAKNESSES, AND APPLICATIONS OF TYPICAL MOR TECHNIQUES FOR THE PHYSICS-BASED LI-ION BATTERY MANAGEMENT

MOR Category	Typical MOR Techniques	Strengths	Weaknesses	Applications of ROMs in Advanced BMS				
				SOC/Electrochem. State Estimation	SOH/Parameter Estimation	Real-Time Charging Control	Charging Profile Optimization	Others
Spatial Discretization	FDM	Easy to implement, generic to all operating conditions	High computation, not mass conservative	[38], [70]–[72]	[73]	[52], [74], [75]	–	–
	FVM, Control Volume Method	Easy to implement, generic to all operating conditions, mass conservative	High computation	[37], [76]	[77]	[78]	[79]	–
Function Approximation	Spectral Methods (e.g. Galerkin Method, Orthogonal Collocation)	Low computation for smooth profiles	Derivation and implementation are complex	[45]	[80], [81]	[49], [82]	[83]	–
	Polynomial Profile Approximation	Easy to implement	Subject to low to medium rates	[37], [84]–[89]	[81], [86], [88]	[33], [75], [78]	[90]	[7] (Renewable energy dispatch)
Frequency Domain Approximation	Eigenfunction Methods	Easy to implement	Linear (small-signal) model	[37], [88]	[88]	–	–	–
	Residual Grouping	High accuracy over wide operating ranges	Need to solve nonlinear optimization problems, linear model	[53]	[91]	[92]	[90], [93]	–
	Padé Approximation	Easy to implement, high accuracy	Linear model	[72], [94]	[94], [95]	[74]	[96], [97]	[98] (HEV energy management)
	Direct Realization Algorithms	Low computation, easy to implement	Linear model, derivation is labor-intensive	[99]	–	[100]	–	–
Simplified Physics/ Spatial Lumping	SPM-Based	Low computation, easy to implement	Narrow operating range, not suitable for high-rate applications	[38], [70], [84], [86], [89], [94], [101]–[103]	[73], [86], [94], [101], [103]	[82]	[97], [104]	[32] (Fault diagnosis)
	ESPM-Based (improved with electrolyte model)	Low computation, enhanced accuracy at higher rates	Not suitable for cells with wide electrodes	[28], [72], [85]	[28], [30]	[33]	[90], [96], [105]	[98] (HEV energy management)

B. Long-Term Prediction of Degraded Performance

Although physics-based models are promising in predicting battery charging/discharging behavior and providing health- and safety-related information for the control system under a wide range of operational conditions, their capability to accurately predict the battery's long-term aging trajectory and remaining lifetime needs further investigation and evaluation. Indeed, over the last two decades, degradation mechanisms have been intensively investigated, however, the quantification of all the aging mechanisms and development of battery degradation models regardless of cell chemistries are an active ongoing research area. In view of recent advancements in big data and artificial intelligence, data-driven modeling enabled by various machine learning techniques is considered to be a favorable approach [108]. In the past few years, a large number of data-driven SOH estimation and remaining useful life prediction models have emerged with the use of the methods such as artificial neural networks [109], Bayesian nonparametric algorithms [110], and support vector machines [111]. These models work well when sufficient battery health data are available but may suffer from scalability problems due to cell-to-cell variations. In [108], Severson *et al.* developed a comprehensive dataset from 169 commercial Li-ion battery cells cycled under 72 different fast-charging conditions. The data were used to classify the cells at very early stages using machine learning, in which the prior knowledge of battery degradation mechanisms was ignored. The authors have reported error rates of less than 10%. As physics-based models can provide more interpretable information for feature extraction, hybridization of physics-based and data-driven modeling techniques [112], potentially with the incorporation of implantable sensing technologies [113] for enhanced internal state observability, shall bring fruitful research outcomes for the development of future health-aware battery management strategies.

C. Parameterization

Parameter identification for physics-based battery models lays a foundation for accurate state estimation and optimal control design. Due to the complexity of high-order physical models and the presence of a large set of parameters, the task of parameter identification is very challenging. It has been theoretically shown that the P2D model and many of its ROMs are over-parameterized [114], [115], so it is impossible to simultaneously identify all the model parameters. Furthermore, many parameters are weakly identifiable from current and voltage measurements. In light of these two aspects, it is necessary to conduct sensitivity analysis, parameter grouping, and optimal experimental designs. Parameter grouping for a given model requires a detailed analysis of the model structure and a theoretical study on the identifiability [114]. Clearly, the parameterization problem would become even more challenging when a large number of cells with different characteristics are considered in a pack configuration and only pack-level measurements are available. Interestingly, for the physics-based equivalent circuits as shown in Figs. 4 and 6, since the circuit parameters such as the resistances and capacitances are always expressed as functions of the electrochemical parameters, intrinsic grouping schemes have been established to simplify the parameter estimation [35]. In addition, the model parameters can be significantly affected by factors such as cell temperature and

pack geometry. Nonuniform temperature distribution on a large battery pack can lead to a heterogeneity problem which can cause inconsistency of battery parameters across the cells and the pack. Overall, the parameterization of a coupled electrochemical and thermal model for lifelong battery management is still an open and active area of research.

VI. Conclusions

Physics-based models can be considered to be the core of sophisticated health- and safety-aware algorithms for next-generation BMSs for Li-ion batteries. To simplify the model complexity, many model order reduction (MOR) approaches for the electrochemical models of Li-ion batteries have been proposed for the next-generation BMSs. Such prominent MOR approaches are categorized as spatial discretization, function approximation, frequency-domain approximation, and simplified physics/spatial lumping methods. Selecting the most appropriate battery MOR techniques to develop health- and safety-aware control algorithms for a particular application is crucial to achieving enhanced battery performance and extended battery lifetime. The chosen reduced-order model needs to have the ability to incorporate aging effects, temperature variations, environmental impacts, and operating conditions. Due to the highly complex physical dynamics inside the Li-ion battery cell and significantly different operating conditions in various applications, combining several MOR techniques is inevitable to develop a state-of-the-art reduced-order Li-ion battery model for a specific BMS functionality. Detailed simulation studies of the full-order battery model are needed before the selection of specific MOR techniques. More efforts have to be made to achieve pack-level modeling with the consideration of cell inconsistency, efficient model parameterization, and long-term aging prediction, possibly through hybridization with data-driven techniques such as machine learning.

Abbreviations

BMS	Battery management system	P2D	Pseudo-two-dimensional
DAE	Differential-algebraic equation	PDE	Partial differential equation
ECM	Equivalent circuit model	PDAE	Partial differential algebraic equation
ESPM	Extended single particle model	ROM	Reduced-order model
EV	Electric vehicle	SEI	Solid-electrolyte interphase
FDM	Finite difference method	SOC	State of charge
FVM	Finite volume method	SOH	State of health
MOR	Model order reduction	SPM	Single particle model
HEV	Hybrid electric vehicle	ODE	Ordinary differential equation

Acknowledgments

This work was supported in part by EU-funded Marie Skłodowska-Curie Actions Individual Fellowships under Grant 895337-BatCon-H2020-MSCA-IF-2019, and in part by Swedish Research Council under Grant 2019-04873.

REFERENCES

[1] X. Hu, C. Zou, C. Zhang, and Y. Li, "Technological developments in batteries: A survey of principal roles, types, and management needs," *IEEE Power Energy Mag.*, vol. 15, no. 5, pp. 20–31, Sep.-Oct. 2017.

[2] X.-G. Yang, Y. Leng, G. Zhang, S. Ge, and C.-Y. Wang, "Modeling of lithium plating induced aging of lithium-ion batteries: Transition from linear to nonlinear aging," *J. Power Sources*, vol. 360, pp. 28–40, Aug. 2017.

[3] H. Rahimi-Eichi, U. Ojha, F. Baronti, and M. Chow, "Battery management system: An overview of its application in the smart grid and electric vehicles," *IEEE Ind. Electron. Mag.*, vol. 7, no. 2, pp. 4–16, Jun. 2013.

[4] M. Berecibar, I. Gandiaga, I. Villarreal, N. Omar, J. van Mierlo, and P. van den Bossche, "Critical review of state of health estimation methods of Li-ion batteries for real applications," *Renew. Sustain. Energy Rev.*, vol. 56, pp. 572–587, Apr. 2016.

[5] K. Li, F. Wei, K. J. Tseng, and B. Soong, "A practical lithium-ion battery model for state of energy and voltage responses prediction incorporating temperature and ageing effects," *IEEE Trans. Ind. Electron.*, vol. 65, no. 8, pp. 6696–6708, Aug. 2018.

[6] Z. Wei, J. Zhao, R. Xiong, G. Dong, J. Pou, and K. J. Tseng, "Online estimation of power capacity with noise effect attenuation for lithium-ion battery," *IEEE Trans. Ind. Electron.*, vol. 66, no. 7, pp. 5724–5735, Jul. 2019.

[7] Y. Li, M. Vilathgamuwa, S. S. Choi, B. Xiong, J. Tang, Y. Su *et al.*, "Design of minimum cost degradation-conscious lithium-ion battery energy storage system to achieve renewable power dispatchability," *Appl. Energy*, vol. 260, p. 114282, Feb. 2020.

[8] S. Xie, X. Hu, Q. Zhang, X. Lin, B. Mu, and H. Ji, "Aging-aware co-optimization of battery size, depth of discharge, and energy management for plug-in hybrid electric vehicles," *J. Power Sources*, vol. 450, p. 227638, Feb. 2020.

[9] X. Hu, K. Zhang, K. Liu, X. Lin, S. Dey, and S. Onori, "Advanced fault diagnosis for lithium-ion battery systems: A review of fault mechanisms, fault features, and diagnosis procedures," *IEEE Ind. Electron. Mag.*, vol. 14, no. 3, pp. 65–91, Sep. 2020.

[10] R. Gu, P. Malysz, H. Yang, and A. Emadi, "On the suitability of electrochemical-based modeling for lithium-ion batteries," *IEEE Trans. Transport. Electrific.*, vol. 2, no. 4, pp. 417–431, Dec. 2016.

[11] U. Krewer, F. Röder, E. Harinath, R. D. Braatz, B. Bedürftig, and R. Findeisen, "Dynamic models of Li-ion batteries for diagnosis and operation: A review and perspective," *J. Electrochem. Soc.*, vol. 165, no. 16, pp. A3656–A3673, Jan. 2018.

[12] M. T. Lawder, B. Suthar, P. W. C. Northrop, S. De, C. M. Hoff, O. Leitermann *et al.*, "Battery energy storage system (BESS) and battery management system (BMS) for grid-scale applications," *Proc. IEEE*, vol. 102, no. 6, pp. 1014–1030, Jun. 2014.

[13] A. Seaman, T.-S. Dao, and J. McPhee, "A survey of mathematics-based equivalent-circuit and electrochemical battery models for hybrid and electric vehicle simulation," *J. Power Sources*, vol. 256, pp. 410–423, Jul. 2014.

[14] N. A. Chaturvedi, R. Klein, J. Christensen, J. Ahmed, and A. Kojic, "Algorithms for advanced battery-management systems," *IEEE Control Syst. Mag.*, vol. 30, no. 3, pp. 49–68, Jun. 2010.

[15] S. Kolluri, S. V. Aduru, M. Pathak, R. D. Braatz, and V. R. Subramanian, "Real-time nonlinear model predictive control (NMPC) strategies using physics-based models for advanced lithium-ion battery management system (BMS)," *J. Electrochem. Soc.*, vol. 167, no. 6, p. 063505, Apr. 2020.

[16] M. Doyle, T. F. Fuller, and J. Newman, "Modeling of galvanostatic charge and discharge of the lithium/polymer/insertion cell," *J. Electrochem. Soc.*, vol. 140, no. 6, pp. 1526–1533, Jan. 1993.

[17] T. F. Fuller, M. Doyle, and J. Newman, "Simulation and optimization of the dual lithium ion insertion cell," *J. Electrochem. Soc.*, vol. 141, no. 1, pp. 1–10, 1994.

[18] M. Doyle and J. Newman, "Modeling the performance of rechargeable lithium-based cells: Design correlations for limiting cases," *J. Power Sources*, vol. 54, no. 1, pp. 46–51, Mar. 1995.

[19] Y. Li, M. Vilathgamuwa, T. Farrell, S. S. Choi, N. T. Tran, and J. Teague, "A physics-based distributed-parameter equivalent circuit model for lithium-ion batteries," *Electrochim. Acta*, vol. 299, pp. 451–469, Mar. 2019.

[20] M. Torchio, L. Magni, R. B. Gopaluni, R. D. Braatz, and D. M. Raimondo, "LIONSIMBA: A Matlab framework based on a finite volume model suitable for Li-ion battery design, simulation, and control," *J. Electrochem. Soc.*, vol. 163, no. 7, pp. A1192–A1205, Jan. 2016.

[21] V. R. Subramanian, V. Boovaragavan, V. Ramadesigan, and M. Arabandi, "Mathematical model reformulation for lithium-ion battery simulations: Galvanostatic boundary conditions," *J. Electrochem. Soc.*, vol. 156, no. 4, pp. A260–A271, Apr. 2009.

[22] M. Safari and C. Delacourt, "Modeling of a commercial graphite/$LiFePO_4$ cell," *J. Electrochem. Soc.*, vol. 158, no. 5, pp. A562–A571, May 2011.

[23] M. Guo and R. E. White, "A distributed thermal model for a Li-ion electrode plate pair," *J. Power Sources*, vol. 221, pp. 334–344, Jan. 2013.

[24] J. Sturm, S. Ludwig, J. Zwirner, C. Ramirez-Garcia, B. Heinrich, M. F. Horsche *et al.*, "Suitability of physicochemical models for embedded systems regarding a nickel-rich, silicon-graphite lithium-ion battery," *J. Power Sources*, vol. 436, p. 226834, Oct. 2019.

[25] J. M. Reniers, G. Mulder, and D. A. Howey, "Review and performance comparison of mechanical-chemical degradation models for lithium-ion batteries," *J. Electrochem. Soc.*, vol. 166, no. 14, pp. A3189–A3200, Sep. 2019.

[26] B. Wu, W. D. Widanage, S. Yang, and X. Liu, "Battery digital twins: Perspectives on the fusion of models, data and artificial intelligence for smart battery management systems," *Energy and AI*, vol. 1, p. 100016, Aug. 2020.

[27] K. A. Smith, C. D. Rahn, and C.-Y. Wang, "Control oriented 1D electrochemical model of lithium ion battery," *Energy Convers. Manage.*, vol. 48, no. 9, pp. 2565–2578, Sep. 2007.

[28] A. Allam and S. Onori, "Online capacity estimation for lithium-ion battery cells via an electrochemical model-based adaptive interconnected observer," *IEEE Trans. Control Syst. Technol.*, vol. 29, no. 4, pp. 1636–1651, Jul. 2021.

[29] L. Zheng, J. Zhu, G. Wang, D. D. Lu, and T. He, "Lithium-ion battery instantaneous available power prediction using surface lithium concentration of solid particles in a simplified electrochemical model," *IEEE Trans. Power Electron.*, vol. 33, no. 11, pp. 9551–9560, Nov. 2018.

[30] Z. T. Gima, D. Kato, R. Klein, and S. J. Moura, "Analysis of online parameter estimation for electrochemical Li-ion battery models via reduced sensitivity equations," in *Proc. Amer. Control Conf.*, Denver, CO, USA, 1–3 Jul. 2020, pp. 373–378.

[31] A. Pozzi, M. Zambelli, A. Ferrara, and D. M. Raimondo, "Balancing-aware charging strategy for series-connected lithium-ion cells: A nonlinear model predictive control approach," *IEEE Trans. Control Syst. Technol.*, vol. 28, no. 5, pp. 1862–1877, Sep. 2020.

[32] M. A. Rahman, S. Anwar, and A. Izadian, "Electrochemical model based fault diagnosis of a lithium ion battery using multiple model adaptive estimation approach," in *Proc. IEEE Int. Conf. Ind. Technol.*, Seville, Spain, 17-19 Mar. 2015, pp. 210–217.

[33] C. Zou, X. Hu, Z. Wei, T. Wik, and B. Egardt, "Electrochemical estimation and control for lithium-ion battery health-aware fast charging," *IEEE Trans. Ind. Electron.*, vol. 65, no. 8, pp. 6635–6645, Aug. 2018.

[34] M.-T. von Srbik, M. Marinescu, R. F. Martinez-Botas, and G. J. Offer, "A physically meaningful equivalent circuit network model of a lithium-ion battery accounting for local electrochemical and thermal behaviour, variable double layer capacitance and degradation," *J. Power Sources*, vol. 325, pp. 171–184, Sep. 2016.

[35] Y. Merla, B. Wu, V. Yufit, R. F. Martinez-Botas, and G. J. Offer, "An easy-to-parameterise physics-informed battery model and its application towards lithium-ion battery cell design, diagnosis, and degradation," *J. Power Sources*, vol. 384, pp. 66–79, Apr. 2018.

[36] M. Corno, "Efficient control-oriented coupled electrochemical thermal modeling of Li-ion cells," *IEEE Trans. Ind. Electron.*, vol. 68, no. 8, pp. 7024–7033, Aug. 2021.

[37] J. Sturm, H. Ennifar, S. V. Erhard, A. Rheinfeld, S. Kosch, and A. Jossen, "State estimation of lithium-ion cells using a physicochemical model based extended Kalman filter," *Appl. Energy*, vol. 223, pp. 103–123, Aug. 2018.

[38] D. Di Domenico, A. Stefanopoulou, and G. Fiengo, "Lithium-ion battery state of charge and critical surface charge estimation using an electrochemical model-based extended Kalman filter," *J. Dynamic Syst. Meas. Control*, vol. 132, no. 6, p. 061302, Nov. 2010.

[39] L. Cai and R. E. White, "Reduction of model order based on proper orthogonal decomposition for lithium-ion battery simulations," *J. Electrochem. Soc.*, vol. 156, no. 3, pp. A154–A161, Mar. 2009.

[40] Y. Zeng, P. Albertus, R. Klein, N. Chaturvedi, A. Kojic, M. Z. Bazant *et al.*, "Efficient conservative numerical schemes for 1D nonlinear spherical diffusion equations with applications in battery modeling," *J. Electrochem. Soc.*, vol. 160, no. 9, pp. A1565–A1571, Jan. 2013.

[41] D. Zhang, S. Dey, L. D. Couto, and S. J. Moura, "Battery adaptive observer for a single-particle model with intercalation-induced stress," *IEEE Trans. Control Syst. Technol.*, vol. 28, no. 4, pp. 1363–1377, Jul. 2020.

[42] R. Achar and M. S. Nakhla, "Simulation of high-speed interconnects," *Proc. IEEE*, vol. 89, no. 5, pp. 693–728, May 2001.

[43] W. He, M. Pecht, D. Flynn, and F. Dinmohammadi, "A physics-based electrochemical model for lithium-ion battery state-of-charge estimation solved by an optimised projection-based method and moving-window-filtering," *Energies*, vol. 11, no. 8, p. 2120, 2018.

[44] T.-S. Dao, C. P. Vyasarayani, and J. McPhee, "Simplification and order reduction of lithium-ion battery model based on porous-electrode theory," *J. Power Sources*, vol. 198, pp. 329–337, Jan. 2012.

[45] A. M. Bizeray, S. Zhao, S. R. Duncan, and D. A. Howey, "Lithium-ion battery thermal-electrochemical model-based state estimation using orthogonal collocation and a modified extended Kalman filter," *J. Power Sources*, vol. 296, pp. 400–412, Nov. 2015.

[46] D. W. Limoge, P. Y. Bi, A. M. Annaswamy, and A. Krupadanam, "A reduced-order model of a lithium-ion cell using the absolute nodal coordinate formulation approach," *IEEE Trans. Control Syst. Technol.*, vol. 26, no. 3, pp. 1001–1014, May 2018.

[47] G. Fan, X. Li, and M. Canova, "A reduced-order electrochemical model of Li-ion batteries for control and estimation applications," *IEEE Trans. Veh. Technol.*, vol. 67, no. 1, pp. 76–91, Jan. 2018.

[48] L. Cai and R. E. White, "Lithium ion cell modeling using orthogonal collocation on finite elements," *J. Power Sources*, vol. 217, pp. 248–255, Nov. 2012.

[49] J. Liu, G. Li, and H. K. Fathy, "An extended differential flatness approach for the health-conscious nonlinear model predictive control of lithium-ion batteries," *IEEE Trans. Control Syst. Technol.*, vol. 25, no. 5, pp. 1882–1889, Sep. 2017.

[50] V. R. Subramanian, V. D. Diwakar, and D. Tapriyal, "Efficient macro-micro scale coupled modeling of batteries," *J. Electrochem. Soc.*, vol. 152, no. 10, pp. A2002–A2008, Aug. 2005.

[51] S. Santhanagopalan, Q. Guo, P. Ramadass, and R. E. White, "Review of models for predicting the cycling performance of lithium ion batteries," *J. Power Sources*, vol. 156, no. 2, pp. 620–628, Jun. 2006.

[52] Y. Li, D. M. Vilathgamuwa, E. Wikner, Z. Wei, X. Zhang, T. Thiringer *et al.*, "Electrochemical model-based fast charging: Physical constraint-triggered PI control," *IEEE Trans. Energy Convers.*, in press.

[53] K. A. Smith, C. D. Rahn, and C.-Y. Wang, "Model-based electrochemical estimation and constraint management for pulse operation of lithium ion batteries," *IEEE Trans. Control Syst. Technol.*, vol. 18, no. 3, pp. 654–663, May 2010.

[54] H. Zhao, M. Hong, W. Lin, and K. A. Loparo, "Voltage and frequency regulation of microgrid with battery energy storage systems," *IEEE Trans. Smart Grid*, vol. 10, no. 1, pp. 414–424, Jan. 2019.

[55] S. Khaleghi Rahimian, S. Rayman, and R. E. White, "Extension of physics-based single particle model for higher chargedischarge rates," *J. Power Sources*, vol. 224, pp. 180–194, Feb. 2013.

[56] M. Guo and R. E. White, "An approximate solution for solid-phase diffusion in a spherical particle in physics-based Li-ion cell models," *J. Power Sources*, vol. 198, pp. 322–328, Jan. 2012.

[57] N. T. Tran, M. Vilathgamuwa, T. Farrell, S. S. Choi, Y. Li, and J. Teague, "A Padé approximate model of lithium ion batteries," *J. Electrochem. Soc.*, vol. 165, no. 7, pp. A1409–A1421, May 2018.

[58] N. T. Tran, M. Vilathgamuwa, T. Farrell, S. S. Choi, and Y. Li, "A computationally efficient coupled electrochemical-thermal model for large format cylindrical lithium ion batteries," *J. Electrochem. Soc.*, vol. 166, no. 13, pp. A3059–A3071, Sep. 2019.

[59] J. L. Lee, A. Chemistruck, and G. L. Plett, "One-dimensional physics-based reduced-order model of lithium-ion dynamics," *J. Power Sources*, vol. 220, pp. 430–448, Dec. 2012.

[60] A. Rodríguez, G. L. Plett, and M. S. Trimboli, "Comparing four model-order reduction techniques, applied to lithium-ion battery-cell internal electrochemical transfer functions," *eTransport.*, vol. 1, p. 100009, Aug. 2019.

[61] A. Rodríguez, G. L. Plett, and M. S. Trimboli, "Improved transfer functions modeling linearized lithium-ion battery-cell internal electrochemical variables," *J. Energy Storage*, vol. 20, pp. 560–575, Dec. 2018.

[62] Y. Li, M. Vilathgamuwa, S. S. Choi, T. W. Farrell, N. T. Tran, and J. Teague, "Development of a degradation-conscious physics-based lithium-ion battery model for use in power system planning studies," *Appl. Energy*, vol. 248, pp. 512–525, Aug. 2019.

[63] J. M. Reniers, G. Mulder, and D. A. Howey, "Unlocking extra value from grid batteries using advanced models," *J. Power Sources*, vol. 487, p. 229355, Mar. 2021.

[64] R. Klein, N. A. Chaturvedi, J. Christensen, J. Ahmed, R. Findeisen, and A. Kojic, "Electrochemical model based observer design for a lithium-ion battery," *IEEE Trans. Control Syst. Technol.*, vol. 21, no. 2, pp. 289–301, Jan. 2011.

[65] J. Marcicki, M. Canova, A. T. Conlisk, and G. Rizzoni, "Design and parametrization analysis of a reduced-order electrochemical model of graphite/$LiFePO_4$ cells for SOC/SOH estimation," *J. Power Sources*, vol. 237, pp. 310–324, Sep. 2013.

[66] S. J. Moura, F. B. Argomedo, R. Klein, A. Mirtabatabaei, and M. Krstic, "Battery state estimation for a single particle model with electrolyte dynamics," *IEEE Trans. Control Syst. Technol.*, vol. 25, no. 2, pp. 453–468, Mar. 2017.

[67] J. Newman, "Fortran programs for the simulation of electrochemical systems." [Online]. Available: http://www.cchem.berkeley.edu/jsngrp/fortran.html

[68] S. Moura, "FastDFN: Fast Doyle-Fuller-Newman (DFN) electrochemical-thermal battery model simulator," 2018. [Online]. Available: https://github.com/scott-moura/fastDFN

[69] V. Sulzer, S. G. Marquis, R. Timms, M. Robinson, and S. J. Chapman, "Python battery mathematical modelling (PyBaMM)," *J. Open Res. Softw.*, vol. 9, no. 1, p. 14, Jun. [Online]. Available: https://github.com/pybamm-team/PyBaMM

[70] S. Dey, B. Ayalew, and P. Pisu, "Nonlinear robust observers for state-of-charge estimation of lithium-ion cells based on a reduced electrochemical model," *IEEE Trans. Control Syst. Technol.*, vol. 23, no. 5, pp. 1935–1942, Sep. 2015.

[71] S. Marelli and M. Corno, "Model-based estimation of lithium concentrations and temperature in batteries using soft-constrained dual unscented Kalman filtering," *IEEE Trans. Control Syst. Technol.*, vol. 29, no. 2, pp. 926–933, Mar. 2021.

[72] W. Li, Y. Fan, F. Ringbeck, D. Jöst, X. Han, M. Ouyang *et al.*, "Electrochemical model-based state estimation for lithium-ion batteries with adaptive unscented Kalman filter," *J. Power Sources*, vol. 476, p. 228534, Nov. 2020.

[73] R. Ahmed, M. E. Sayed, I. Arasaratnam, J. Tjong, and S. Habibi, "Reduced-order electrochemical model parameters identification and SOC estimation for healthy and aged Li-ion batteries Part I: Parameterization model development for healthy batteries," *IEEE J. Emerg. Sel. Topics Power Electron.*, vol. 2, no. 3, pp. 659–677, Sep. 2014.

[74] H. Perez, N. Shahmohammadhamedani, and S. Moura, "Enhanced performance of Li-ion batteries via modified reference governors and electrochemical models," *IEEE/ASME Trans. Mechatronics*, vol. 20, no. 4, pp. 1511–1520, Aug. 2015.

[75] C. Zou, C. Manzie, and D. Nešić, "Model predictive control for lithium-ion battery optimal charging," *IEEE/ASME Trans. Mechatronics*, vol. 23, no. 2, pp. 947–957, Apr. 2018.

[76] Y. Li, B. Xiong, D. M. Vilathgamuwa, Z. Wei, C. Xie, and C. Zou, "Constrained ensemble Kalman filter for distributed electrochemical state estimation of lithium-ion batteries," *IEEE Trans. Ind. Inform.*, vol. 17, no. 1, pp. 240–250, Jan. 2021.

[77] T. R. Ashwin, A. McGordon, W. D. Widanage, and P. A. Jennings, "Modified electrochemical parameter estimation of NCR18650BD battery using implicit finite volume method," *J. Power Sources*, vol. 341, pp. 387–395, Feb. 2017.

[78] A. Pozzi, M. Torchio, R. D. Braatz, and D. M. Raimondo, "Optimal charging of an electric vehicle battery pack: A real-time sensitivity-based model predictive control approach," *J. Power Sources*, vol. 461, p. 228133, Jun. 2020.

[79] M. Torchio, L. Magni, R. D. Braatz, and D. M. Raimondo, "Optimal health-aware charging protocol for lithium-ion batteries: A fast model predictive control approach," *IFAC-PapersOnLine*, vol. 49, no. 7, pp. 827–832, Jan. 2016.

[80] V. Ramadesigan, K. Chen, N. A. Burns, V. Boovaragavan, R. D. Braatz, and V. R. Subramanian, "Parameter estimation and capacity fade analysis of lithium-ion batteries using reformulated models," *J. Electrochem. Soc.*, vol. 158, no. 9, p. A1048, Jul. 2011.

[81] D. W. Limoge and A. M. Annaswamy, "An adaptive observer design for real-time parameter estimation in lithium-ion batteries," *IEEE Trans. Control Syst. Technol.*, vol. 28, no. 2, pp. 505–520, Mar. 2020.

[82] M. S. S. Malik, G. Li, and Z. Chen, "An optimal charging algorithm to minimise solid electrolyte interface layer in lithium-ion battery," *J. Power Sources*, vol. 482, p. 228895, Jan. 2021.

[83] H. E. Perez, S. Dey, X. Hu, and S. J. Moura, "Optimal charging of Li-ion batteries via a single particle model with electrolyte and thermal dynamics," *J. Electrochem. Soc.*, vol. 164, no. 7, pp. A1679–A1687, Jun. 2017.

[84] N. Lotfi, R. G. Landers, J. Li, and J. Park, "Reduced-order electrochemical model-based SOC observer with output model uncertainty estimation," *IEEE Trans. Control Syst. Technol.*, vol. 25, no. 4, pp. 1217–1230, Jul. 2017.

[85] X. Hu, D. Cao, and B. Egardt, "Condition monitoring in advanced battery management systems: Moving horizon estimation using a reduced electrochemical model," *IEEE/ASME Trans. Mechatronics*, vol. 23, no. 1, pp. 167–178, Feb. 2018.

[86] B. Jenkins, A. Krupadanam, and A. M. Annaswamy, "Fast adaptive observers for battery management systems," *IEEE Trans. Control Syst. Technol.*, vol. 28, no. 3, pp. 776–789, May 2020.

[87] M. K. S. Verma, S. Basu, R. S. Patil, K. S. Hariharan, S. P. Adiga, S. M. Kolake *et al.*, "On-board state estimation in electrical vehicles: Achieving accuracy and computational efficiency through an electrochemical model," *IEEE Trans. Veh. Technol.*, vol. 69, no. 3, pp. 2563–2575, Mar. 2020.

[88] B. Liu, X. Tang, and F. Gao, "Joint estimation of battery state-of-charge and state-of-health based on a simplified pseudo-two-dimensional model," *Electrochim. Acta*, vol. 344, p. 136098, Jun. 2020.

[89] Y. Liu, R. Ma, S. Pang, L. Xu, D. Zhao, J. Wei *et al.*, "A nonlinear observer SOC estimation method based on electrochemical model for lithium-ion battery," *IEEE Trans. Ind. Appl.*, vol. 57, no. 1, pp. 1094–1104, Jan.–Feb. 2021.

[90] Y. Yin, Y. Hu, S.-Y. Choe, H. Cho, and W. T. Joe, "New fast charging method of lithium-ion batteries based on a reduced order electrochemical model considering side reaction," *J. Power Sources*, vol. 423, pp. 367–379, May 2019.

[91] Y. Bi, Y. Yin, and S.-Y. Choe, "Online state of health and aging parameter estimation using a physics-based life model with a particle filter," *J. Power Sources*, vol. 476, p. 228655, Nov. 2020.

[92] Y. Yin and S.-Y. Choe, "Actively temperature controlled health-aware fast charging method for lithium-ion battery using nonlinear model predictive control," *Appl. Energy*, vol. 271, p. 115232, Aug. 2020.

[93] M. Song and S.-Y. Choe, "Fast and safe charging method suppressing side reaction and lithium deposition reaction in lithium ion battery," *J. Power Sources*, vol. 436, p. 226835, Oct. 2019.

[94] A. Bartlett, J. Marcicki, S. Onori, G. Rizzoni, X. G. Yang, and T. Miller, "Electrochemical model-based state of charge and capacity estimation for a composite electrode lithium-ion battery," *IEEE Trans. Control Syst. Technol.*, vol. 24, no. 2, pp. 384–399, Mar. 2016.

[95] X. Zhang, J. Lu, S. Yuan, J. Yang, and X. Zhou, "A novel method for identification of lithium-ion battery equivalent circuit model parameters considering electrochemical properties," *J. Power Sources*, vol. 345, pp. 21–29, Mar. 2017.

[96] Y. Gao, X. Zhang, B. Guo, C. Zhu, J. Wiedemann, L. Wang *et al.*, "Health-aware multiobjective optimal charging strategy with coupled electrochemical-thermal-aging model for lithium-ion battery," *IEEE Trans. Ind. Inform.*, vol. 16, no. 5, pp. 3417–3429, May 2020.

[97] S. Park, D. Lee, H. J. Ahn, C. Tomlin, and S. Moura, "Optimal control of battery fast charging based-on Pontryagin's minimum principle," in *Proc. IEEE Conf. Decis. Control*, Jeju, South Korea, 14–18 Dec. 2020, pp. 3506–3513.

[98] L. De Pascali, F. Biral, and S. Onori, "Aging-aware optimal energy management control for a parallel hybrid vehicle based on electrochemical-degradation dynamics," *IEEE Trans. Veh. Technol.*, vol. 69, no. 10, pp. 10 868–10 878, Oct. 2020.

[99] K. D. Stetzel, L. L. Aldrich, M. S. Trimboli, and G. L. Plett, "Electrochemical state and internal variables estimation using a reduced-order physics-based model of a lithium-ion cell and an extended Kalman filter," *J. Power Sources*, vol. 278, pp. 490–505, Mar. 2015.

[100] M. A. Xavier, A. K. d. Souza, K. Karami, G. L. Plett, and M. S. Trimboli, "A computational framework for lithium ion cell-level model predictive control using a physics-based reduced-order model," *IEEE Control Syst. Lett.*, vol. 5, no. 4, Oct. 2021.

[101] S. K. Rahimian, S. Rayman, and R. E. White, "State of charge and loss of active material estimation of a lithium ion cell under low earth orbit condition using Kalman filtering approaches," *J. Electrochem. Soc.*, vol. 159, no. 6, pp. A860–A872, Jan. 2012.

[102] R. Ahmed, M. E. Sayed, I. Arasaratnam, J. Tjong, and S. Habibi, "Reduced-order electrochemical model parameters identification and state of charge estimation for healthy and aged Li-ion batteries–Part II: Aged battery model and state of charge estimation," *IEEE J. Emerg. Sel. Topics Power Electron.*, vol. 2, no. 3, pp. 678–690, Sep. 2014.

[103] S. J. Moura, N. A. Chaturvedi, and M. Krstic, "Adaptive partial differential equation observer for battery state-of-charge/state-of-health estimation via an electrochemical model," *J. Dyn. Syst. Meas. Control*, vol. 136, no. 1, p. 011015, Jan. 2014.

[104] X. Lin, X. Hao, Z. Liu, and W. Jia, "Health conscious fast charging of Li-ion batteries via a single particle model with aging mechanisms," *J. Power Sources*, vol. 400, pp. 305–316, Oct. 2018.

[105] F. Lam, A. Allam, W. T. Joe, Y. Choi, and S. Onori, "Offline multiobjective optimization for fast charging and reduced degradation in lithium-ion battery cells using electrochemical dynamics," *IEEE Control Syst. Lett.*, vol. 5, pp. 2066–2071, Dec. 2021.

[106] F. Feng, X. Hu, L. Hu, F. Hu, Y. Li, and L. Zhang, "Propagation mechanisms and diagnosis of parameter inconsistency within Li-ion battery packs," *Renew. Sustain. Energy Rev.*, vol. 112, pp. 102–113, Sep. 2019.

[107] W. Han, T. Wik, A. Kersten, G. Dong, and C. Zou, "Next-generation battery management systems: Dynamic reconfiguration," *IEEE Ind. Electron. Mag.*, vol. 14, no. 4, pp. 20–31, Dec. 2020.

[108] K. A. Severson, P. M. Attia, N. Jin, N. Perkins, B. Jiang, Z. Yang *et al.*, "Data-driven prediction of battery cycle life before capacity degradation," *Nature Energy*, vol. 4, no. 5, pp. 383–391, May 2019.

[109] Y. Tan and G. Zhao, "Transfer learning with long short-term memory network for state-of-health prediction of lithium-ion batteries," *IEEE Trans. Ind. Electron.*, vol. 67, no. 10, pp. 8723–8731, Oct. 2020.

[110] X. Tang, C. Zou, K. Yao, J. Lu, Y. Xia, and F. Gao, "Aging trajectory prediction for lithium-ion batteries via model migration and Bayesian Monte Carlo method," *Appl. Energy*, vol. 254, p. 113591, Nov. 2019.

[111] J. Wei, G. Dong, and Z. Chen, "Remaining useful life prediction and state of health diagnosis for lithium-ion batteries using particle filter and support vector regression," *IEEE Trans. Ind. Electron.*, vol. 65, no. 7, pp. 5634–5643, Jul. 2018.

[112] M. Aykol, C. B. Gopal, A. Anapolsky, P. K. Herring, B. van Vlijmen, M. D. Berliner *et al.*, "Perspective—Combining physics and machine learning to predict battery lifetime," *J. Electrochem. Soc.*, vol. 168, no. 3, p. 030525, Mar. 2021.

[113] Z. Wei, J. Zhao, H. He, G. Ding, H. Cui, and L. Liu, "Future smart battery and management: Advanced sensing from external to embedded multi-dimensional measurement," *J. Power Sources*, vol. 489, p. 229462, Mar. 2021.

[114] A. M. Bizeray, J. Kim, S. R. Duncan, and D. A. Howey, "Identifiability and parameter estimation of the single particle lithium-ion battery model," *IEEE Trans. Control Syst. Technol.*, vol. 27, no. 5, pp. 1862–1877, Sep. 2019.

[115] Z. Chu, R. Jobman, A. Rodríguez, G. L. Plett, M. S. Trimboli, X. Feng *et al.*, "A control-oriented electrochemical model for lithium-ion battery. Part II: Parameter identification based on reference electrode," *J. Energy Storage*, vol. 27, p. 101101, Feb. 2020.

Yang Li (yangli@ieee.org) received the Ph.D. degree in power engineering from Nanyang Technological University, Singapore, in 2015. He is currently a Researcher with the Department of Electrical Engineering, Chalmers University of Technology, Gothenburg, Sweden. His research interests include modeling and control of battery systems in grid systems and transport sector. Dr. Li was a recipient of the EU Marie Skłodowska-Curie Action Individual Fellowship for battery research in 2020.

Dulmini Karunathilake (r.ralahamilage@qut.edu.au) received her B.Sc. degree in electrical and electronic engineering from the University of Peradeniya, Sri Lanka, in 2015. She is currently pursuing her Ph.D. degree at the School of Electrical Engineering and Robotics, Queensland University of Technology, Brisbane, QLD, Australia. Her areas of interest are lithium-ion battery modelling, battery management systems, and health-conscious optimal control of lithium-ion batteries.

D. Mahinda Vilathgamuwa (mahinda.vilathgamuwa@qut.edu.au) holds the Ph.D. degree from the University of Cambridge, Cambridge, UK, and currently serves as professor of power engineering at Queensland University of Technology, Brisbane, QLD, Australia. His research interests are on battery modeling and control, wireless power transfer, and electromobility.

Yateendra Mishra (yateendra.mishra@qut.edu.au) received the Ph.D. degree in electrical engineering from the University of Queensland, Brisbane QLD, Australia, in 2009. He is currently a Senior Lecturer and Advance QLD Research Fellow with the School of Electrical Engineering and Robotics, Queensland University of Technology, Brisbane, QLD, Australia. His current research interests include distributed energy generation, distributed energy storage, power system stability and control, and their applications in smart grid.

Troy W. Farrell (t.farrell@qut.edu.au) received the Ph.D. degree in mathematics from the Queensland University of Technology, Brisbane, QLD, Australia, in 1998, where he is currently a Professor with the School of Mathematical Sciences. His research interests include industrial and applied mathematical modeling and simulation, electrochemical systems, and multiscale porous media.

San Shing Choi (sanshing.choi@qut.edu.au) received the Ph.D. degree in electrical engineering from the University of Canterbury, Christchurch, New Zealand, in 1976. He was previously with the New Zealand Electricity Department, Wellington, New Zealand, National University of Singapore, the State Energy Commission of Western Australia, and Nanyang Technological University, Singapore. He is currently an Adjunct Professor with the Curtin University of Technology, Perth, and Queensland University of Technology, Brisbane, both in Australia. His research interests include power system control, renewable, and energy storage systems.

Changfu Zou (changfu.zou@chalmers.se) received his Ph.D. degree in automation and control engineering from the University of Melbourne, Australia, in 2017. He is an Assistant Professor in the Automatic Control Group, Chalmers University of Technology, Gothenburg, Sweden. His research interests include the intelligent management of energy systems and electric vehicles. He serves as an editor of IEEE Transactions on Vehicular Technology and an associate editor of IEEE Transactions on Transportation Electrification.